

ESFuelCell2012-91362

A QUASI STEADY STATE MODEL FOR ADSORPTION COOLING SYSTEMS: AUTOMOTIVE APPLICATIONS

Amirhossein Sharafianardakani

PhD Candidate

Laboratory for Alternative Energy Conversion (LAEC),
Mechatronic Systems Engineering,
School of Engineering Science,
Simon Fraser University, BC,
Canada
asharafi@sfu.ca

Majid Bahrami*

Associate Professor

Laboratory for Alternative Energy Conversion (LAEC),
Mechatronic Systems Engineering,
School of Engineering Science,
Simon Fraser University, BC,
Canada
mbahrami@sfu.ca

ABSTRACT

In this study, an analytical quasi-steady state thermodynamic cycle of an adsorption cooling system (ACS) for automotive applications is presented which allows evaluating impact of different parameters on the ACS performance as well as effects of various working pairs: zeolite 13X/water, zeolite 4A/water and activated carbon-35/methanol. A comprehensive parametric study has been performed to investigate effects of temperature variation of the evaporator and condenser as well as the ICE exhaust gas temperature on the COP, cooling load produced by the evaporator and entropy generation of ACS with (or without) the heat recovery cycle (HRC). The results show that using the heat recovery cycle in the ACS can increase the COP of system up to 41% for zeolite 13X/water pair at the base-line condition. In addition, the parametric study shows that increasing regeneration and evaporation temperature increase the COP and entropy generation of ACS while increasing condensation temperature has negative effect on the COP and entropy generation. Finally, based on our modeling results, the ACS with the heat recovery cycle (HRC) and zeolite 13X/water pair are proposed for the automotive A/C applications.

Key words: Adsorption cooling system, thermodynamic cycle, heat recovery cycle, zeolite13X/water.

1. INTRODUCTION

Efficient use of fuel and improving performance are two fundamental goals of the energy management system of advanced vehicles. These topics have received an increasing attention in the recent years due to higher fuel prices, energy shortages, and emerging governmental stringent

environmental/emission regulations. To this end, there has been an immense attention to reduce auxiliary loads in vehicles. Heating ventilating and air-conditioning (HVAC) loads are the most significant auxiliary loads present in internal combustion engine (ICE) vehicles today; its energy use even outweighs the energy loss to rolling resistance, aerodynamic drag, or driveline losses for a typical vehicle. The U.S. consumes about 7 billion gallons of fuel a year for HVAC systems of light duty vehicles [1]. An HVAC compressor can add up to 5-6 kW peak power draw on a vehicle's engine. This power draw is equivalent to a 1200-kg sedan driving steady-state down the road at 60 km/h.

Conventional internal combustion engines reject a significant portion of the fuel energy in the form of low-grade thermal energy or waste heat and converting only a portion of the fuel energy into the useful mechanical energy [2]. Hence, there is a significant opportunity to utilize this waste heat to run the air conditioner of vehicle using a thermally-driven adsorption cooling system (ACS), and immensely increase the overall vehicle efficiency. In addition, ACS refrigerants, called adsorbates, are usually environment friendly, non-corrosive, and non-toxic fluids [3]. Water and methanol are common adsorbates in the ACS which are readily accessible and inexpensive. Furthermore, the ACS adsorbents, such as silica gel, activated carbon and zeolite, can operate in different operating pressures and temperatures and are inexpensive and environment friendly.

The ACS, in essence, operates similar to the vapor compression refrigeration cycle with the exception that the compressor is replaced by packed bed(s) of adsorbent. Hence, the ACS has no moving parts and does not need regular maintenance which makes it a great candidate for automotive A/C application [4]. However, there are major challenges

facing commercialization of the ACS including their low coefficient of performance (COP) and, more importantly, low specific cooling power (SCP) in comparison with the conventional cooling systems. These drawbacks lead to the ACS' bulky size and heavy weight [5].

Developing an accurate thermodynamic model that can predict the behavior of ACS under various operating conditions using different adsorption pairs is the first step to build a real ACS. The present work can then be used in design and optimization purposes. The following provides a review on the pertinent models available in the literature.

Cassiola *et al.* [6] presented a quasi-steady state model for three different working pairs: activated carbon-35/methanol, zeolite 4A/water and zeolite 13X/water. Their model was one of the pioneer works in this field that can predict the COP of ACS with/without heat recovery cycle (HRC) under different operating conditions. Hajji and Khalloufi [7] followed the model of Cassiola *et al.* [6] and presented a numerical model to predict the COP as well as temperature distribution in a one dimensional test bed. They, also, verified the model with their experimental data. Their results show that the thickness of adsorbent and the heat transfer coefficient of test bed have a considerable effect on the cooling capacity of ACS. Zhang and Wang [8] developed a non-equilibrium model to predict the COP and SCP of ACS. They mentioned that the SCP is more sensitive to the variation of operating conditions, namely evaporation, condensation and regeneration temperature, than the COP.

Zhang and Wang [9], also, investigated the effects of bed design on the COP and SCP of ACS. Based on their results, permeability of zeolite plays an important role on the mass transfer inside the bed; also, short cycle time significantly limits the performance of ACS. Later, Wu *et al.* [10] investigated the dynamic behavior of ACS experimentally and numerically. The working pair in their experiment was activated carbon/methanol. Their numerical SCP had good agreement with the experimental data, but their numerical COP deviated from the experimental results. Also, Wu *et al.* [11] used a continuous heat recovery ACS which works with the activated carbon/methanol pair. In their experimental work, effects of cycle parameters on the COP and SCP of system were studied. Akahira *et al.* [12] investigated the effects of mass recovery on the silica gel/water ACS. The mass recovery was done by making a pressure gradient between the two beds during adsorption and desorption processes. Their results show that the COP of ACS with mass recovery is higher than that of a simple ACS. However, adding mass recovery increases the complexity of ACS.

Chekirou *et al.* [13] used the model of Cassiola *et al.* [6] for the activated carbon-35/methanol ACS and investigated the effects of heat recovery cycle on the performance. Their results showed that the heat recovery cycle improved the COP of ACS.

The objective of this study is to develop a quasi-steady state thermodynamic cycle that can predict the performance (COP), and the entropy generation of ACS with (or without) heat recovery cycle (HRC) for the automotive A/C applications

under various operating conditions and using different working pairs.

2. THERMODYNAMIC CYCLE OF AN ADSORPTION COOLING SYSTEM

Thermodynamic cycle of an ACS includes four main processes: i) isosteric heating (constant specific volume), ii) isobaric desorption, iii) isosteric cooling, and iv) isobaric adsorption. As Fig. 1 shows, the ACS is similar to the vapor compression refrigeration cycle except the compressor is replaced with the adsorption beds. Therefore, the major components of ACS are adsorber beds, condenser, expansion valve, and evaporator.

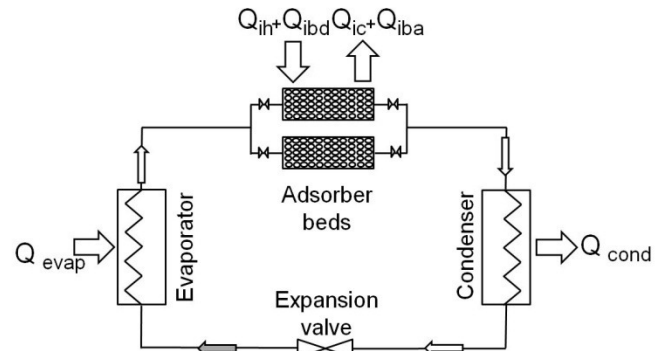


Fig. 1: Schematic of an adsorption cooling system.

Figure 2 shows the thermodynamic cycle of an adsorption system for the adsorbate (working fluid) and adsorbent cycles on a Clapeyron diagram.

During step 1-2, adsorber through an isosteric process, absorbs heat in amount of Q_{ih} from an external heat source (isosteric heating). In this step, the adsorbent and adsorbate are heated and the pressure and temperature of adsorber bed increases. This process will be continued until the pressure of the adsorber bed reaches the pressure of condenser. At this time, the entrance valve to the condenser will be opened [4].

In step 2-3', the external heat source is continuing to transfer heat to the adsorber bed (Q_{ibd}) during an isobaric desorption process and the adsorbate is extracted from the adsorbent and is cooled by the condenser during an isobaric cooling process (step 2-3). In this step, gaseous adsorbate loses its heat (Q_{cond}) and condenses to liquid [4].

After heating of the adsorbent up to the point 3' which is the maximum temperature of cycle, the valve between the adsorber bed and the condenser will be closed and during an isosteric cooling process, the adsorbent loses its heat (Q_{ic}) in contact with a heat sink during step 3'-4' [4].

In step 3-4, the adsorbate passes through the expansion valve and, during a constant enthalpy process, the liquid adsorbate expands to a saturated mixture of vapor and liquid [4].

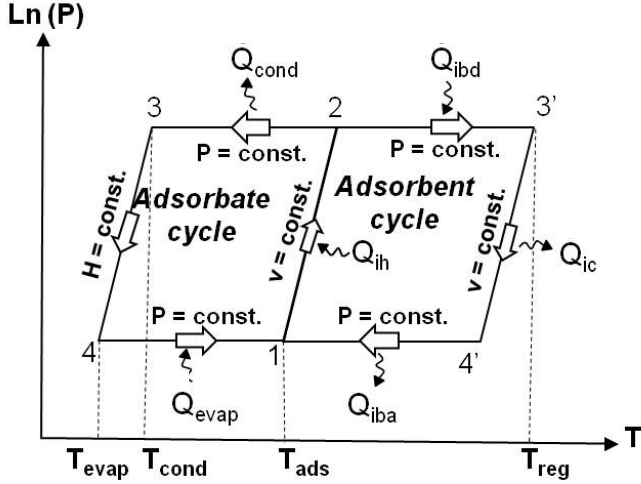


Fig. 2: Thermodynamic cycle of an adsorption cooling system on a Clapeyron diagram.

In step 4-1, the adsorbate absorbs heat in an amount of Q_{evap} from the environment and converts to the vapor. At the same time, the entrance valve to the adsorber bed will be opened and the adsorbent adsorbs the vapor adsorbate during an isobaric adsorption (step 4'-1) and releases its heat (Q_{iba}) [4].

3. THERMODYNAMIC MODEL

In this study, a quasi-state thermodynamic model is developed based on a single-bed ACS; it is then extended to a two-bed ACS with heat recovery cycle (HRC) following the work of [6]. It is assumed that the amount of adsorbate that is in equilibrium with the adsorbent is a function of operating temperature and pressure. Moreover, the enthalpy of adsorption is just a function of the adsorbate uptake which is generally calculated from the equilibrium condition under the specific pressure and temperature. The adsorption-equilibrium equation for the adsorbent-adsorbate pair is presented in Eq. (1) [6].

$$\ln(P) = a(\omega) + \frac{b(\omega)}{T} \quad (1)$$

$$a(\omega) = a_0 + a_1\omega + a_2\omega^2 + a_3\omega^3 \quad (2)$$

$$b(\omega) = M_i \frac{\Delta H_a}{R_u} = b_0 + b_1\omega + b_2\omega^2 + b_3\omega^3 \quad (3)$$

where ω is the amount of adsorbate uptake within the adsorbent in kg/kg dried adsorbent, T is the adsorbent temperature in K , P is the pressure of the adsorber in $mbar$ and the constant coefficients a_i and b_i are reported in Table 1 for three different adsorbent-adsorbate pairs: zeolite 4A/water, zeolite 13X/water and activated carbon-35/methanol [6]. ΔH_a is the heat of adsorption in $J/kg.K$ which is calculated by Eq. (3), M_i is the

molar mass of adsorbate in kg/mol and R_u is the universal gas constant in $J/mol.K$. The heat of adsorption is physically different from the enthalpy of vaporization. It is larger than the enthalpy of vaporization due to the Van der Waals bonding between the adsorbate and adsorbent [14].

To calculate the saturation pressure as a function of temperature, Eq. (4) is presented in which a_s and b_s are constant coefficients and their value is 20.5896 and -5098.26 for water, and 20.84 and -4696.0 for methanol, respectively [6].

$$\ln(P_s) = a_s + \frac{b_s}{T} \quad (4)$$

where T is the temperature of the adsorbate in K and P_s is the saturation pressure in $mbar$.

Thermo-physical properties of the adsorbate (water and methanol), the specific heat of liquid and vapor adsorbate, and the latent heat of vaporization for the pure adsorbate, are expressed as functions of temperature as follows [15,16].

$$c_{p,lw} = 5 \times 10^{-5} T^3 - 0.0465 T^2 + 13.476 T + 2884.0 \quad (5)$$

$$c_{p,wv} = 0.006 T^2 - 0.0426 T + 1824.1 \quad (6)$$

$$h_{fg,w} = -0.0071 T^2 + 2.6204 T + 2286.6 \quad (7)$$

$$c_{p,lm} = 6.3 T + 287.8 \quad (8)$$

$$c_{p,mv} = 2.4016 T + 657.21 \quad (9)$$

$$h_{fg,m} = -0.0107 T^2 + 5.2034 T + 554.15 \quad (10)$$

The specific heats of adsorbent and adsorber bed are assumed to be constant: 836.0 $J/kg.K$ for the zeolite, 920.0 $J/kg.K$ for the activated carbon, and 470.0 $J/kg.K$ for the adsorber bed [8,17].

The amount of sensible heat that should be transferred to the adsorber bed during the isosteric heating, Q_{ih} , is,

$$Q_{ih} = (m_z(c_{p,z} + c_{p,li}\omega_{max}) + m_{bed}c_{p,bed})(T_2 - T_1) \quad (11)$$

where i is water or methanol and ω_{max} is the maximum amount of the adsorbate uptake by the adsorbent at T_{ads} during the isosteric heating process. In this step, it is assumed that the adsorbate is in the liquid phase and there is no phase change.

The amount of heat transfer to the adsorber bed during the isobaric desorption process is obtained by Eq. (12).

$$Q_{ibd} = (m_z(c_{p,z} + \bar{\omega}c_{p,li}) + m_{bed}c_{p,bed})(T_{3'} - T_2) + m_z \int_{\omega_{max}}^{\omega_{min}} \Delta H_a d\omega \quad (12)$$

Table 1: Constant coefficients, a_i and b_i , in the adsorbent-adsorbate equilibrium equation [5,18].

	a_0	a_1	a_2	a_3	b_0	b_1	b_2	b_3
zeolite 4A/water	14.8979	95.408	-636.66	1848.8	-7698.85	21498.1	-184598.0	512605.0
zeolite 13X/water	13.4244	110.854	-731.76	1644.8	-7373.78	6722.92	5624.47	-3486.7
activated carbon-35/methanol	20.3305	6.53035	-16.6841	52.3793	-6003.58	6315.16	-26058.7	40537.9

where $\bar{\omega}$ is $\frac{\omega_{max} + \omega_{min}}{2}$. As it is seen, the heat transfer includes the sensible heat and the latent heat (enthalpy of adsorption) which results from the phase change of the adsorbate from the liquid phase to the vaporous phase. During the isobaric desorption process, the vapor adsorbate leaves the adsorber bed toward the condenser, please see Fig. 2.

Removed sensible heat from the adsorber bed during the isosteric cooling process is calculated by Eq. (13).

$$Q_{ic} = (m_z (c_{p,z} + c_{p,li}\omega_{min}) + m_{bed}c_{p,bed})(T_4' - T_3') \quad (13)$$

And, finally, the energy balance during the isobaric adsorption is equal to the sensible heat resulting from the cooling of adsorbent plus the enthalpy of adsorption minus the heat gained by the adsorbate from the evaporation to the adsorption temperature [6].

$$Q_{iba} = (m_z (c_{p,z} + \bar{\omega}c_{p,li}) + m_{bed}c_{p,bed})(T_1 - T_4') + m_z \int_{\omega_{min}}^{\omega_{max}} \Delta H_a d\omega + Q_{hva} \quad (14)$$

$$Q_{hva} = m_z c_{p,iv@T_e} \sum_{j=1}^n (\omega_j - \omega_{j-1}) \left(0.5 \left(\frac{b(\omega_j)}{\ln(P_e) - a(\omega_j)} + \frac{b(\omega_{j-1})}{\ln(P_e) - a(\omega_{j-1})} \right) - T_e \right) \quad (15)$$

where i is water or methanol, $n = \frac{\omega_{max} - \omega_{min}}{k}$ and $k \ll 1$ is a constant related to the accuracy of the model. In this study, its value is assumed 10^{-6} .

The released heat from the condenser is,

$$Q_{cond} = m_z (\omega_{max} - \omega_{min}) h_{fg@T_c} + Q_{cvc} \quad (16)$$

$$Q_{cvc} = m_z c_{p,iv@T_c} \sum_{j=1}^n (\omega_j - \omega_{j-1}) \left(0.5 \left(\frac{b(\omega_j)}{\ln(P_c) - a(\omega_j)} + \frac{b(\omega_{j-1})}{\ln(P_c) - a(\omega_{j-1})} \right) - T_c \right) \quad (17)$$

where i is water or methanol and Q_{cvc} is the sensible heat of vaporous adsorbate which is being cooled from the desorption to the condenser temperature.

The cooling load that can be generated by the evaporator during the isobaric adsorption consists of the latent heat of evaporation of working fluid minus the sensible heat of adsorbate that is entering to the evaporator at the temperature of condenser, Eq. (18).

$$Q_{evap} = m_z (\omega_{max} - \omega_{min}) (h_{fg@T_e} - c_{p,li}(T_c - T_e)) \quad (18)$$

To have a better understanding of the cooling load under different operating conditions, normalized evaporation cooling load, Eq. (19), is defined as a function of evaporator cooling load at the base-line condition; please see Table 3 and 4.

$$Q_{evap}^* = \frac{Q_{evap}}{Q_{evap,base-line}} \quad (19)$$

The COP of ACS is the ratio of the cooling effect produced at the evaporator to the total supplied heat.

$$COP = \frac{Q_{evap}}{Q_{ih} + Q_{ibd}} \quad (20)$$

By adding a heat recovery cycle (HRC) to the simple ACS, one can transfer removed heat during the isosteric cooling and isobaric adsorption (steps 3'-4' and 4'-1) to the isosteric heating and isobaric desorption processes (steps 1-2 and 2-3'). To maximize the effects of HRC, the amount of heat gain during the steps 1-3', Q_{rd} , in a specific temperature, T_{HRC} , and the released heat during the steps 3'-1, Q_{ra} , at that temperature must be equal. For the desorption process, Q_{rd} is calculated by Eqs. (21) and (22).

If $T_1 < T < T_2$:

$$Q_{rd} = (m_z (c_{p,z} + c_{p,li}\omega_{max}) + m_{bed}c_{p,bed})(T - T_1) \quad (21)$$

For $T_2 < T < T_3$:

$$Q_{rd} = Q_{ih} + (m_z (c_{p,z} + \bar{\omega}c_{p,li}) + m_{bed}c_{p,bed})(T - T_2) + m_z \int_{\omega_{max}}^{\omega} \Delta H_a d\omega \quad (22)$$

For the adsorption process, Eqs. (23) and (24) gives Q_{ra} .

If $T_4' < T < T_3$:

$$Q_{ra} = (m_z (c_{p,z} + c_{p,li}\omega_{min}) + m_{bed}c_{p,bed})(T - T_3') \quad (23)$$

For $T_1 < T < T_4$:

$$Q_{ra} = Q_{ic} + (m_z (c_{p,z} + \bar{\omega}c_{p,li}) + m_{bed}c_{p,bed})(T - T_4') + m_z \int_{\omega_{min}}^{\omega} \Delta H_a d\omega + Q_{hva} \quad (24)$$

The maximum effect of the HRC will happen, where $Q_{rd} = |Q_{ra}|$. At this point, the temperature of T_{HRC} , and the recovered heat of Q_{HRC} , can be calculated. Accordingly, the coefficient of performance is calculated by the following,

$$COP_{HRC} = \frac{Q_{evap}}{Q_{ih} + Q_{ibd} - Q_{HRC}} \quad (25)$$

The ACS is a closed thermodynamic cycle which just exchanges heat with its surrounding. Therefore, the total entropy generation throughout the whole cycle results from the heat transfers to and from the adsorber beds, condenser and evaporator. As a result, entropy generation in the ACS is simply calculated by the following:

$$S_{gen} = -\left(\frac{Q_{ih} + Q_{ibd}}{T_{reg}} + \frac{Q_{ic} + Q_{iba}}{T_{amb}} + \frac{Q_{cond}}{T_{cond}} + \frac{Q_{evap}}{T_{evap}} \right) \quad (26)$$

where Q_{ih} , Q_{ibd} and Q_{evap} are positive values while Q_{ic} , Q_{iba} and Q_{cond} are negative. Based on the first law of thermodynamics, the total heat transfer to and from the thermal-driven closed thermodynamic cycle of ACS is equal to

zero. Thus, the first law of thermodynamics for the ACS without HRC is,

$$Q_{ih} + Q_{ibd} + Q_{ic} + Q_{iba} + Q_{cond} + Q_{evap} = 0 \quad (27)$$

By substituting Eqs. (20) and (27) in Eq. (26), the non-dimensional entropy generation of ACS without the HRC is calculated by Eq. (28).

$$S_{gen}^* = \frac{T_{reg} S_{gen}}{Q_{ih} + Q_{ibd}} = - \left[\left(1 - \frac{T_{reg}}{T_{amb}}\right) + \frac{T_{reg} Q_{cond}}{Q_{ih} + Q_{ibd}} \left(\frac{1}{T_{cond}} - \frac{1}{T_{amb}}\right) + COP T_{reg} \left(\frac{1}{T_{evap}} - \frac{1}{T_{amb}}\right) \right] \quad (28)$$

The entropy generation in the ACS with the HRC will be lower than that of the ACS without the HRC due to the heat recovery between the adsorber beds which decreases the amount of total heat transfer to and from the adsorber beds of ACS. Eq. (29) gives the total entropy generation of the ACS with the HRC.

$$S_{gen,HRC} = - \left(\frac{Q_{ih} + Q_{ibd} - Q_{HRC}}{T_{reg}} + \frac{Q_{ic} + Q_{iba} + Q_{HRC}}{T_{amb}} + \frac{Q_{cond}}{T_{cond}} + \frac{Q_{evap}}{T_{evap}} \right) \quad (29)$$

where Q_{HRC} is a positive value. Similar to Eq. (28), the non-dimensional entropy generation is calculated by Eq. (30).

$$S_{gen,HRC}^* = \frac{T_{reg} S_{gen,HRC}}{Q_{ih} + Q_{ibd} - Q_{HRC}} = - \left[\left(1 - \frac{T_{reg}}{T_{amb}}\right) + \frac{T_{reg} Q_{cond}}{Q_{ih} + Q_{ibd}} \left(\frac{1}{T_{cond}} - \frac{1}{T_{amb}}\right) + COP_{HRC} T_{reg} \left(\frac{1}{T_{evap}} - \frac{1}{T_{amb}}\right) \right] \quad (30)$$

4. RESULTS AND DISCUSSION

4.1. COMPARISON

To verify the developed thermodynamic cycle of ACS, variation of the regeneration temperature on the cooling load and the COP of ACS for three different working pairs: zeolite 13X/water, zeolite 4A/water and activated carbon-35/methanol are compared against the numerical results of Cacciola *et al.* [6]. Table 2 shows the operating conditions reported in the numerical thermodynamic model presented by Cacciola *et al.* [6].

Table 2: Operating conditions in [6] to verify the present work.

Parameter	value
Evaporation temperature, T_{evap}	5°C
Condensation temperature, T_{cond}	40°C
Adsorption temperature, T_{ads}	40°C
Adsorbent mass, m_z	1kg
Mass of adsorber bed, m_{bed}	Not reported

Figure 3 shows the effects of regeneration temperature on the cooling load of ACS for the three different working pairs.

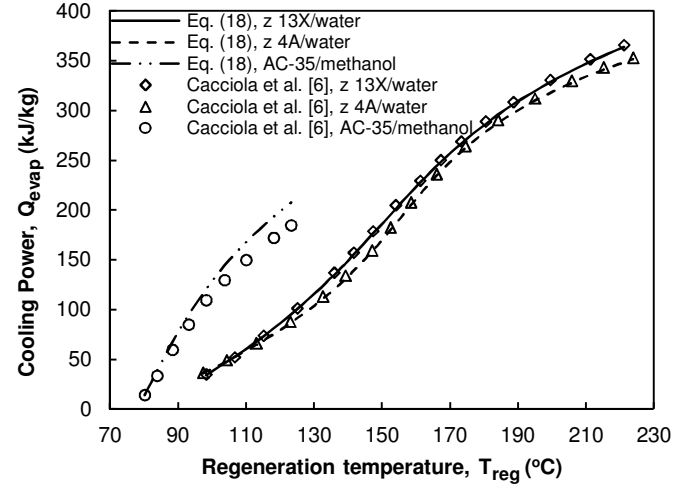


Fig. 3: Effect of regeneration temperature on the cooling load of ACS for the three different working pairs compared against the reported values by [6], see Table 2.

The present work shows a good agreement with the numerical results of Cacciola *et al.* [6] with a maximum and average relative differences of 2.2% and 1.1% for the zeolite 13X/water pair, 2.9% and 1.5% for the zeolite 4A/water, and 14% and 10.7% for the activated carbon-35/methanol, respectively.

Figure 3, also, indicates that the regeneration temperature has a considerable effect on the cooling load of ACS. In addition, since the zeolite 13X/water and zeolite 4A/water pairs can work at higher temperatures than the activated carbon-35/methanol pair, the cooling load produced by the ACS can be higher when the zeolite /water is used at higher temperatures. However, at the low temperatures, the activated carbon-35/methanol pair yields higher cooling load in comparison with the zeolite/ water pair.

Furthermore, the effects of regeneration temperature on the COP_{HRC} of ACS are compared against the reported results by Cacciola *et al.* [6] in Fig. 4.

The maximum and average relative differences between the present work and the reported results by Cacciola *et al.* [6] are 8.4% and 4.5% for the zeolite 13X/water, 9.6% and 5% for the zeolite 4A/water, and 11.3% and 6.4% for the activated carbon-35/methanol, respectively.

As Fig. 4 shows, the activated carbon-35/methanol pair has higher COP in temperatures below 150°C but it cannot be used in higher temperatures due to the methanol dissociation at temperatures higher than 150°C. To use the activated carbon/methanol ACS, cascading ACS is recommended which can operate with two different working pairs, namely a combination of zeolite/water and activated carbon/methanol pairs; the first cycle works with the high temperature heat source and the second cycle works with the released heat from the first cycle.

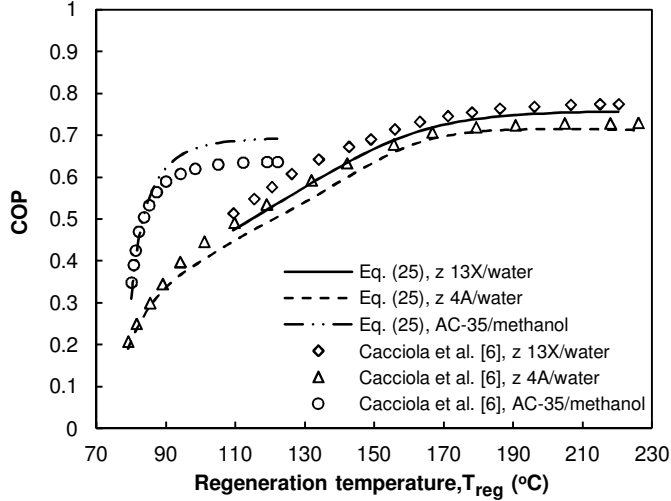


Fig. 4: Effect of regeneration temperature on the COP of ACS for the three different working pairs compared against the reported values by [6], see Table 2.

For the automotive A/C applications, the exhaust gas of ICE has the temperature range of 200-400°C [19]. Therefore, using the zeolite 13X/water as a working pair in the ACS can provide more cooling load as well as COP. Moreover, the zeolite 13X has a good thermal stability and its adsorption capacity only decreases by 20% after 3500 cycles [20]. As a result, it can be concluded that the zeolite 13X/water ACS is a promising candidate for using the automotive applications due to the high stability, COP and cooling load. The following provides effects of different operating conditions on the COP, cooling load and entropy generation of zeolite 13X/water ACS with (or without) HRC.

4.2. PARAMETRIC STUDY

In order to adopt the ACS in the automotive A/C applications, the cycle time which limits continuous cooling supply should be improved. The Adsorbate flow rate inside the cycle changes with the time, thus to provide the better COP as well as acceptable cooling load, the operating temperature in different parts of the ACS should be set in such a way that can provide comfortable conditions in the vehicle. For the automotive A/C application, Table 3 lists base-line conditions for the ACS with zeolite 13X/water pair. These conditions are recommended in the numerical model presented by Zhang *et al.* [8] for the automotive A/C application.

Table 3: Base-line operating conditions of the ACS for automotive A/C application [8].

Parameter	value
Adsorption temperature, T_{ads}	80°C
Regeneration temperature, T_{reg}	240°C
Evaporation temperature, T_{evap}	10°C
Condensation temperature, T_{cond}	45°C
Ambient temperature, T_{amb}	35°C
Adsorbent mass, m_z	15kg
Mass of adsorber bed, m_{ped}	6 kg

The thermodynamic results at the base-line conditions are presented in Table 4.

Table 4: Thermodynamic results of ACS in the base-line conditions for the zeolite 13X/water pair.

Parameter	value
Q_{ih}	1270.6 kJ
Q_{ibd}	8124.7 kJ
Q_{ic}	-1283.7 kJ
Q_{iba}	-7302.4 kJ
Q_{evap}	4296.5 kJ
Q_{cond}	-4905.0 kJ
Q_{hr}	2815.5 kJ
COP	0.46
COP_{HRC}	0.65
S_{gen}	9.8 kJ/K
$S_{gen,HRC}$	6.15 kJ/K

Table 4 shows adding a heat recovery cycle to the ACS increases the COP of system from 0.46 to 0.65 (more than 41%). In addition, the entropy generation of ACS with the HRC decreases by 37% than that of ACS without the HRC.

The trend of COP, evaporation cooling load and entropy generation in the ACS with (or without) HRC are investigated with respect to different parameters, namely, regeneration temperature, condensation, evaporation and adsorption temperatures as well as the heat capacity of adsorber bed and adsorbent mass. In all cases, the operating conditions are fixed at the base-line conditions (see Table 3) and only one parameter is changed.

Figure 5 shows the effects of regeneration temperature, T_{reg} , on the COP, cooling load and entropy generation of the ACS with (or without) HRC.

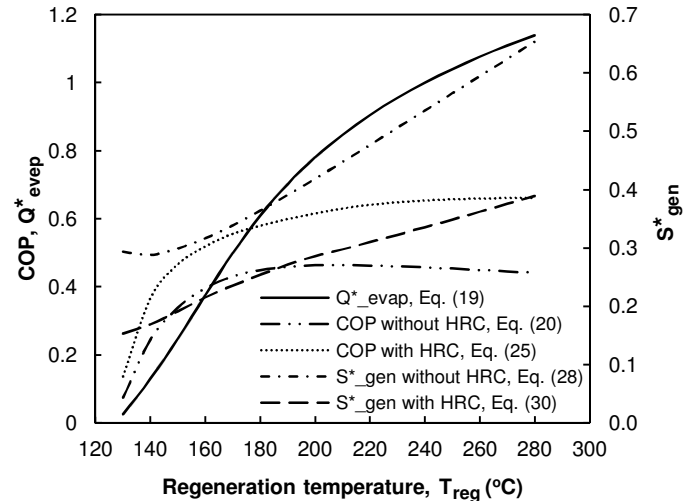


Fig. 5: COP, cooling load and entropy generation of the ACS with/without the HRC versus regeneration temperature. All operating parameters are fixed at the base-line conditions listed in Table 3.

Figure 5 shows that the impact of regeneration temperature is important on the performance of ACS and considerably changes the output of system. The cooling load of evaporator increases sharply with the regeneration temperature. In the regeneration temperature range of 200-280°C, the cooling load increases more than 100%. Also, the COP of ACS without HRC increases with the regeneration temperature and has a maximum at the regeneration temperature of 210°C. In addition, the ACS with the HRC increases steadily with the regeneration temperature and has a higher COP than the ACS without the HRC. Figure 5 indicates that the COP_{HRC} is 41% higher than the COP at the same regeneration temperature of 240°C. Besides, it can be seen that the COP of ACS with HRC enhances sharply with the regeneration temperature but its growth from 240 to 280°C is less than 1%.

Figure 5 shows the entropy generation increases with respect to the regeneration temperature. Furthermore, it can be seen that the HRC effectively decreases the entropy generation in the ACS which is mainly due to decreasing the amount of heat transfer to and from the system. The entropy generation of ACS with the HRC is 59% lower than that of ACS without the HRC. Therefore, adding the HRC can maximize the COP and minimize the entropy generation. Based on Fig. 5, one can conclude that, for automotive A/C applications, the regeneration temperature of 240°C can provide a relatively high COP (0.46 for the ACS without the HRC and 0.65 for the ACS with the HRC) and cooling load as well as lower entropy generation than the higher regeneration temperatures.

Effects of condensation temperature on the COP, evaporation cooling load and entropy generation of the ACS are shown in Fig. 6.

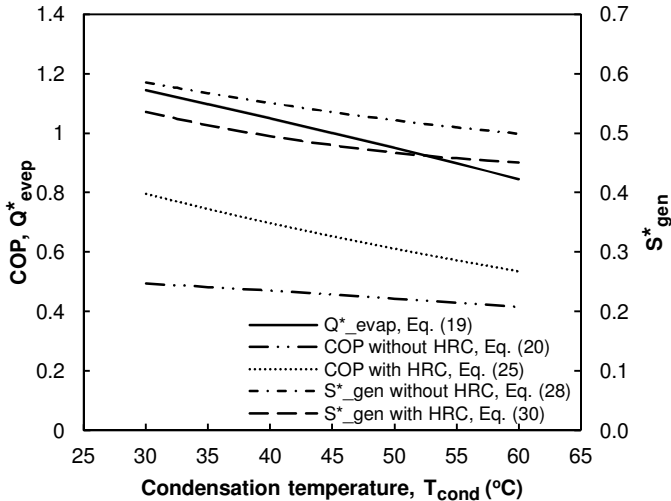


Fig. 6: COP, cooling load and entropy generation of the ACS with/without the HRC versus condensation temperature. All operating parameters are fixed at the base-line conditions, see Table 3.

Figure 6 indicates that increasing the condensation temperature from 30 to 60°C, decreases the cooling load about 21% and the COP of ACS without the HRC will decrease from

0.49 to 0.41 while the COP of ACS with HRC decreases considerably from 0.8 to 0.54. Besides, the entropy generation decreases with increasing the condensation temperature. Increasing the condensation temperature from 30 to 60°C decreases the entropy generation by 11% and 12% for the ACS with and without the HRC, respectively.

The effects of evaporation temperature on the COP, cooling load and entropy generation of the ACS are shown in Fig. 7.

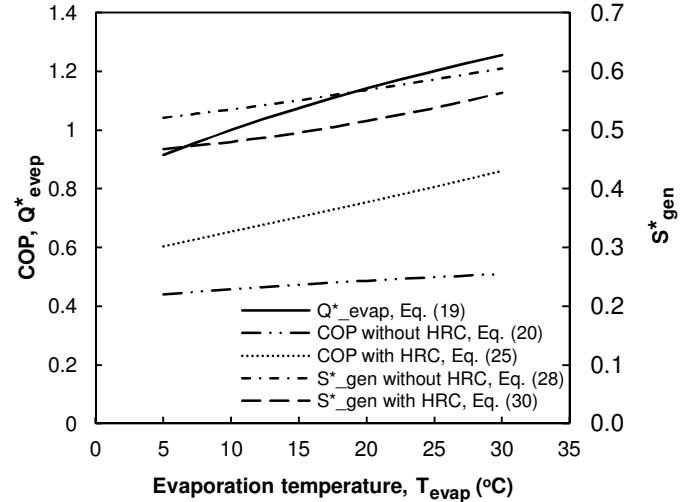


Fig. 7: COP, cooling load and entropy generation of the ACS with/without the HRC versus evaporation temperature. All operating parameters are fixed at the base-line conditions, see Table 3.

Figure 7 shows that by increasing the evaporation temperature, the evaporation cooling load increases which results from higher adsorbate uptake, ω_{max} , and, as a result, higher adsorbate flow rate. Figure 7, also, indicates that increasing the evaporation temperature has more effect on the COP_{HRC} than the COP. It is worth to mention that, for the automotive A/C applications, the evaporation temperature should be set less than 12°C in order to achieve the passengers' comfortable temperature range of 20-23°C [21].

Furthermore, Fig. 7 shows that the entropy generation increases by increasing the evaporation temperature. However, the amount of entropy generation in the ACS with the HRC is lower than that of the ACS without the HRC.

The effects of adsorption temperature on the COP, cooling load and entropy generation of the ACS with (or without) the HRC is shown in Fig. 8. Figure 8 indicates that the cooling load of evaporator is affected considerably by the adsorption temperature. The cooling load decreases about 31% by increasing the adsorption temperature from 50 to 90°C.

Figure (8), also, shows that the COP_{HRC} and the COP reduce steadily by increasing the adsorption temperature. Similarly, the adsorption temperature has no significant effect on the entropy generation of ACS.

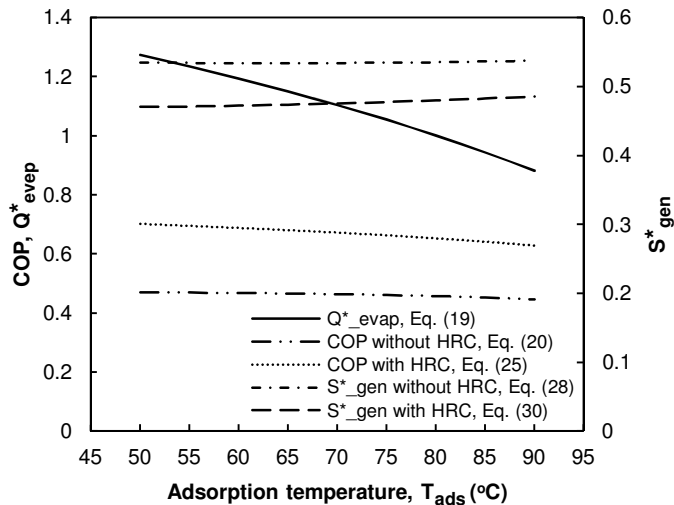


Fig. 8: COP, cooling load and entropy generation of the ACS with/without the HRC versus adsorption temperature. All operating parameters are fixed at the base-line conditions, see Table 3.

The effects of adsorber bed heat capacity on the COP, cooling load and entropy generation of the ACS with (or without) the HRC is shown in Fig. 9.

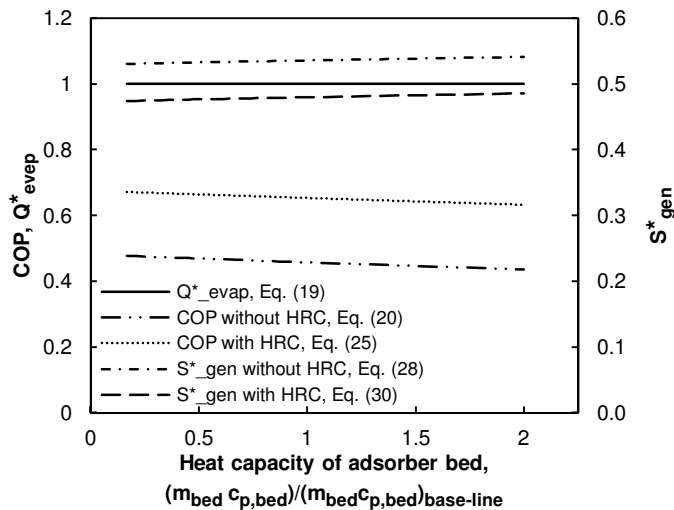


Fig. 9: COP, cooling load and entropy generation of the ACS with/without the HRC versus heat capacity of the adsorber bed. All operating parameters are fixed at the base-line conditions, see Table 3.

Figure 9 shows that the heat capacity of adsorber bed has not considerable effect on the cooling load and entropy generation of ACS. While, increasing the heat capacity of adsorber bed decreases the COP_{HRC} from 0.67 to 0.63 and the COP from 0.47 to 0.43, see Fig. 9.

Figure 10 shows the COP, cooling load of evaporator and entropy generation of the ACS versus the adsorbent mass.

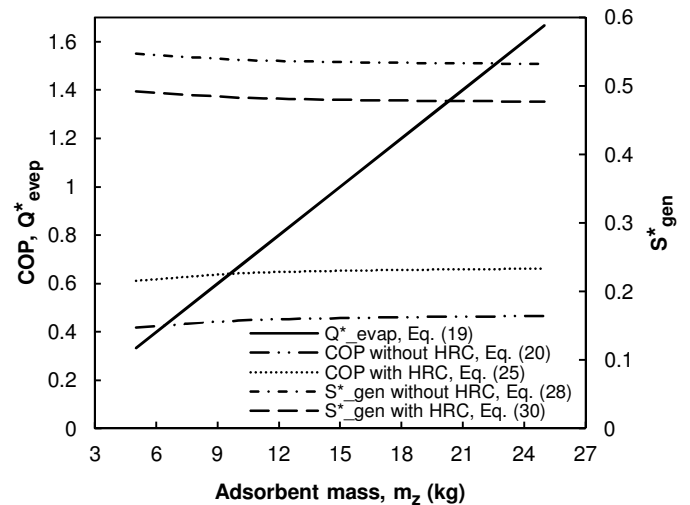


Fig. 10: COP, cooling load and entropy generation of the ACS with/without the HRC versus adsorbent mass. All operating parameters are fixed at the base-line conditions, see Table 3.

Figure 10 indicates that the COP and non-dimensional entropy generation do not change with the adsorbent mass while the cooling load highly affects by that and increases linearly as the adsorbent mass increases.

5. CONCLUSION

In this study, a quasi-steady state thermodynamic model of the ACS with (or without) the HRC for automotive A/C applications was developed for three different working pairs: zeolite 4A/water, zeolite 13X/water and activated carbon-35/methanol. The present study was verified with the numerical results of Cacciola *et al.* [6] and the results showed a good agreement with the reported data of [6].

Due to the higher stability, COP and cooling load of zeolite 13X/water pair at high operating temperatures, it was selected as the working pair in the ACS for the automotive A/C applications. Effects of variation of operating conditions on the ACS with (or without) the HRC showed that,

- Adding the HRC effectively increases the COP and decreases the entropy generation.
- Increasing the regeneration temperature considerably increases the COP, evaporation cooling load and entropy generation.
- Increasing the condensation temperature and decreasing the evaporation temperature decrease the COP, cooling load and entropy generation.
- The adsorption temperature and adsorbent mass have no considerable effect on the COP and non-dimensional entropy generation while the evaporation cooling load increases significantly by these parameters.
- The adsorber bed heat capacity and adsorbent mass have no significant effect on the COP, cooling load and entropy generation.

ACKNOWLEDGMENT

The authors gratefully acknowledge the financial support of the Natural Sciences and Engineering Research Council of Canada (NSERC) through the Automotive Partnership Canada Grant No. APCPJ 401826-10.

NOMENCLATURE

a	constants
b	constants
c_p	specific heat, $J/kg.K$
COP	coefficient of performance
h_{fg}	enthalpy of vaporization, J/kg
ΔH_a	enthalpy of adsorption, $J/kg.K$
Q	heat transfer, kJ
m	mass, kg
M	molar mass, kg/mol
P	pressure, $mbar$
R_u	universal gas constant, $J/mol.K$
S_{gen}	entropy generation, kJ/K
T	temperature, K

Greek symbols

ω	mass of adsorbate inside adsorbent, kg/kg dried adsorbent
----------	----------------------------------------------------------------

Subscript

ads	adsorption
amb	ambient
bed	adsorber bed
c	condenser
$cond$	condensation
cvc	cooling down from desorption to condensation temperature
e	evaporator
$evap$	evaporation
HRC	heat recovery cycle
hva	heat up from evaporation to the adsorption temperature
iba	isobaric adsorption
ibd	isobaric desorption
ic	isosteric cooling
ih	isosteric heating
z	adsorbent
lm	liquid methanol
lw	liquid water
mv	methanol vapor
R	refrigerator
ra	heat recovery during adsorption
rd	heat recovery during desorption
reg	regeneration
s	saturation
wv	water vapor

REFERENCES

[1] R. Farrington, J. Rugh. Impact of vehicle air-conditioning on fuel economy, tailpipe emissions, and electric vehicle range.

Proceeding of the Earth Technologies Forum, Washington, D.C., October 31, 2000.

[2] S. Wang, C. Ji, J. Zhang, B. Zhang. Improving the performance of a gasoline engine with the addition of hydrogen-oxygen mixtures. *International Journal of Hydrogen Energy* (2011); 36: 11164–11173.

[3] M. O. Abdullaha, I. A. W. Tana, L. S. Limb. Automobile adsorption air-conditioning system using oil palm biomass-based activated carbon: A review. *Renewable and Sustainable Energy Reviews* (2011); 15: 2061–2072.

[4] H. Demir, M. Mobedi, S. Ulku. A review on adsorption heat pump: Problems and solutions. *Renewable and Sustainable Energy Reviews* (2008); 12: 2381–2403.

[5] R.Z. Wang, J.Y. Wu, Y.X. Xu, W. Wang. Performance researches and improvements on heat regenerative adsorption refrigerator and heat pump. *Energy Conversion and Management* (2001); 42: 233–249.

[6] G. Cacciola, G. Restuccia. Reversible adsorption heat pump: a thermodynamic model. *International Journal of Refrigeration* (1995); 18(2): 100–106.

[7] A. Hajji, S. Khalloufi. Theoretical and experimental investigation of a constant-pressure adsorption process. *International Journal of Heat and Mass Transfer* (1995); 38(18): 3349–3358.

[8] L.Z. Zhang, L. Wang. Performance estimation of an adsorption cooling system for automobile waste heat recovery. *Applied Thermal Engineering* (1997); 17(12): 1127–1139.

[9] L. Z. Zhang, L. Wang. Effects of coupled heat and mass transfers in adsorbent on the performance of a waste heat adsorption cooling unit. *Applied Thermal Engineering* (1999); 19: 195–215.

[10] J.Y. Wu, R.Z. Wang, Y.X. Xu. Dynamic simulation and experiments of a heat regenerative adsorption heat pump. *Energy Conversion and Management* (2000); 41: 1007–1018.

[11] J.Y. Wu, R.Z. Wang, Y.X. Xu. Experimental results on operating parameters influence for an adsorption refrigerator. *International Journal of Thermal Sciences* (2002); 41: 137–145.

[12] A. Akahira, K. C. A. Alam, Y. Hamamoto, A. Akisawa, T. Kashiwagi. Mass recovery adsorption refrigeration cycle-improving cooling capacity. *International Journal of Refrigeration* (2004); 27: 225–34.

[13] W. Chekiroua, R. Boussehainb, M. Feidtb, A. Karaalia, N. Boukheita. Numerical results on operating parameters influence for a heat recovery adsorption machine. *Energy Procedia* (2011); 6: 202–216.

[14] W. W. Eckenfelder. *Industrial Water Pollution Control*, 3rd edition (1999); McGraw-Hill Science.

[15] Y.A. Cengel, M. Boles. *Thermodynamics: An Engineering Approach*, 4th edition (2001); McGraw-Hill College.

[16] <http://www.engineeringtoolbox.com>

[17] N. B. Amar, L. M. Sun, F. Meunier. Numerical analysis of adsorptive temperature wave regenerative heat pump. *Applied Thermal Engineering* (1996); 16(5): 405–418.

[18] G. Cacciola, G. Restuccia, G.H.W. van Benthem. Influence of the adsorber heat exchanger design on the performance of

the heat pump system. *Applied Thermal Engineering* (1999); 19: 255–269.

[19] P. G. O'Reilly, R. J. Kee, R. Fleck, P. T. McEntee. Two-wire thermocouples: A nonlinear state estimation approach to temperature reconstruction. *Review of Scientific Instruments* (2001); 72(8): 3449–3457.

[20] G. Storch, G. Reichenauer, F. Scheffler, A. Hauer. Hydrothermal stability of pelletized zeolite 13X for energy storage applications. *Adsorption* (2008);14: 275–281.

[21] R. de Dear, G. S. Brager. The adaptive model of thermal comfort and energy conservation in the built environment. *International Journal of Biometeorology* (2001); 45: 100–108.